

Closed-form Approximation for Performance Bound of Finite Blocklength Massive MIMO Transmission

Xiaohu You, *Fellow, IEEE*, Bin Sheng, Yongming Huang, *Senior Member, IEEE*, Wei Xu, *Senior Member, IEEE*, Chuan Zhang, *Senior Member, IEEE*, Dongming Wang, *Senior Member, IEEE*, Pengcheng Zhu, *Senior Member, IEEE*, and Chen Ji

Abstract—It is supposed that ultra-reliable low latency communication (uRLLC) would continue to evolve in the future sixth generation (6G) network, to provide enhanced capability towards extreme connectivity, with the aid of well established multiple-input multiple-output (MIMO) technology. Since the latency constraint can be represented equivalently by the blocklength of a codeword, channel coding theory at a finite blocklength plays an important role in theoretic analysis of uRLLC. Based on Polyanskiy's and Yang's asymptotic results on maximal achievable rate, we first derive the proximate closed-form expressions for the expectation and variance of channel dispersion. Then, the upper bound of average maximal achievable rate is obtained for massive MIMO systems under ideal independent and identically distributed fading channels. Since almost all the fundamental parameters, including the spatial degree-of-freedom (DoF), are considered, this expression can be viewed as a performance bound of the spatiotemporal two-dimension channel coding to some extent. Moreover, it is shown by simulation and analysis, as the DoF goes to infinite, MIMO systems reveals a nature of deterministic transmission, since the average maximal achievable coding rate per antenna can be achieved at each transmission. In this case, the inversely proportional law observed therein implies that the blocklength in the time domain can be further shortened at the expense of spatial DoF. This exchangeability of space and time, to support a given coding rate, paves a solid and feasible road for us to further reduce latency in 6G uRLLC.

Index Terms—Channel coding, Mobile Communication, MIMO.

I. INTRODUCTION

IN the beyond fifth-generation (B5G) mobile communication network, ultra-reliable low latency communications (uRLLC) are designed to support a plethora of mission-critical applications, such as autonomous vehicles and virtual reality, where seamless and reliable data transmission is the key to the feasibility of service [1], [2]. The primary objective of uRLLC, as per the third-generation partnership project (3GPP), is to reduce the latency down to 1 ms and simultaneously guaranteeing reliability higher than 99.999% [3]. On the one hand, driven by the increasingly stringent requirements in the emerging application scenarios [4], further enhanced ability of uRLLC is expected towards 6G TKμ extreme connectivity

[5], i.e., the latency is reduced from the order of ms to μs. On the other hand, new applications such as extended reality (XR) will dissolve the boundary between uRLLC and enhanced mobile broadband (eMBB) [6]. As a result, while error control is conventionally achieved by implementing the hybrid automatic repeat request (HARQ) mechanism, the strict latency constraint in uRLLC excludes multiple retransmissions therein. Additionally, potential new features, such as high data rate, also pose considerable challenges to 6G uRLLC [7]–[9].

Implementing uRLLC relies on short packet length and small transmission time interval, which make channel coding more challenging. Enabled by the spatial freedom provided by MIMO, a spatiotemporal two-dimension (2D) channel coding scheme is proposed in [10], which can flexibly balance the transmission reliability and latency under different scenarios. In the link layer, there are some innovative techniques to achieve uRLLC, such as grant-free access, interface diversity, and radio resource allocation. Specifically, three grant-free access retransmission schemes including reactive, k-repetition, and proactive retransmission were analyzed in [11]. On the other hand, novel computing frameworks and network architecture techniques are attracting much attention. By optimizing task offloading and resource allocation at edge nodes, MEC systems shorten the delay and promise to support various mission-critical applications [12]. By serving each user with multiple links from different nodes, multi-connectivity is regarded as an effective approach to ensure high network availability and reliability [13]. To reduce control-plane latency in handover procedure, anticipatory networks predict the mobility of users according to their mobility pattern and reserve resources proactively [14].

A. Prior Arts

All along, packet error probability ε , blocklength (i.e., codeword size) n , and coding rate R (the number of information bits per complex symbol) are the three fundamental metrics involved in communication systems. They are highly correlated to each other and neither is dispensable, just like the vertexes of a triangle [15]–[17]. In 2010, building upon Dobrushin's and Strassen's asymptotic results, Y. Polyanskiy, H. V. Poor, and S. Verdú presented a new framework with tight bounds on R as a function of n and ε under an additive white Gaussian noise (AWGN) channel [18]. The rationale behind Polyanskiy's approach is that for finite n , the coding rate becomes a random variable parameterized by channel

This work is supported by the National R&D Program of China under Grant 2020YFB1806603. (Corresponding Authors: Xiaohu You and Bin Sheng.)

X. You, B. Sheng, Y. Huang, W. Xu, C. Zhang, D. Wang, and P. Zhu are with National Mobile Communications Research Laboratory, Southeast University, Nanjing 210096, China and Purple Mountain Laboratories, Nanjing 211111, China. (email: {xhyu, sbdt, huangym, wxu, chzhang, wangdm, p.zhu}@seu.edu.cn).

C. Ji is with School of Information Science and Technology, Nantong University, Nantong 226019, China. (email: gwidjin@ntu.edu.cn)

capacity and channel dispersion, where the channel dispersion is also a random variable introduced as a rate penalty to characterize the impact of n . In the sequel, a series of works have extended their results to other kinds of point-to-point channels. In a single-input single-output (SISO), stationary coherent fading channel with additive Gaussian noise, [19] obtained a convenient two-term expression for the channel dispersion which is found to rely highly on the dynamics of the fading process. In [20], the non-asymptotic bounds of the maximum coding rate were presented which is found not to be monotonic with respect to the channel coherence time. Consequently, there exists a coherence time that maximizes the coding rate over noncoherent Rayleigh block-fading channels. Its normal approximation in the high SNR regime was then presented in [25], which provides a tractable formula for us to perform further analysis. The throughput of spectrum sharing networks with rate adaptation is studied in [26] and the closed-form expression for the secondary user activation probability is derived by using the existing results on finite blocklength. Following the Polyanskiy's approach, a series of works have extended this result in single antenna to the field of multiple antennas. The maximal achievable rate of finite blocklength in quasi-static MIMO channels, under mild conditions on the fading distribution, has been provided recently by Yang *et al.* [29]. In [30], the closed-form expressions for the message decoding probabilities as well as the throughput, the expected delay, and the error probability of HARQ setups were derived, for single-input-multiple-output (SIMO) systems. Recently, Collins *et al.* in [31] obtained a channel dispersion formula for the MIMO block-fading channel where the most interesting result is that the normalized dispersion decreases with a growing number of receive antennas.

In practical wireless systems, coherent detection is widely used which requires the receiver to know the channel state information (CSI). Usually, CSI is acquired by sending training pilots at the transmitter. Remarkable literatures have been devoted to address channel estimation problems under the consideration of a finite blocklength. In [32] and [33], a rigorous framework for characterizing the error probability in the uplink and downlink of massive MIMO with finite blocklength was proposed. Based on this framework, upper bounds of error probability are given by using the mismatched scaled nearest-neighbor (SNN) decoding rule, and the saddlepoint approximation was provided for numerical evaluation. In [35], when the channel coherence time exceeds the blocklength interval in a non-ergodic case, the rates were proven to converge to the generalized mutual information subject to an outage probability. Compared with normal approximation, the saddlepoint approximation is observed to be more accurate for the case where the target rate is not close to the mean of the information density [33] [34]. While in general cases, it could be difficult to achieve a concise closed-form expression, when the saddlepoint approximation is used.

B. Main Contributions

The concept of massive MIMO was first proposed by Marzetta in 2010, which envisions more antennas at

transceiver than that of conventional MIMO [36]. So far, massive MIMO has been adopted in 5G, as a key physical-layer technology to meet the demand for higher data capacity for mobile networks. It is supposed that the massive MIMO technique will continue to evolve and more antennas are considered to employ, as the Tera Hertz frequency band is envisioned for future 6G. More antennas would provide more augmented DoFs which leads to some remarkable properties, such as channel hardening and decorrelation.

In this paper, expectation and variance of the maximal achievable rate in a massive MIMO system with finite blocklength are investigated. The channel is assumed to be quasi-static so that random fading coefficients remain constant over the duration of each codeword. This is a typical assumption for uRLLC where the blocklength is usually short enough. We assume no CSI available at the transmitter partly because there can be insufficient time for the receiver to feedback CSI in a frequency division duplex (FDD) system. Moreover, isotropic codewords are assumed due to the lack of CSI information. The normal approximation of maximal achievable rate at finite blocklength is presented in [29] for MIMO systems. However, it is still inconvenient to use it to analyze the impact of the numbers of antennas on the packet error probability, because there is no closed-form formulae to describe their relationships. To circumvent this difficulty, we therefore make some approximations and turn to acquire the expectation and variance of channel dispersion.

The main contributions of this paper are summarized as follows.

- The closed-form expressions for expectation and variance of channel dispersion in a massive MIMO system with independent and identically distributed (i.i.d.) fading channels are derived. Although the results are obtained under the assumption that the number of antennas goes to infinity, it is observed through numerical simulations that they are also accurate for a finite, and even not-too-large, number of antennas case.
- we show that, for a massive MIMO system with M transmit antennas and N receive antennas, there exists an approximate solution to the general relationship among latency n , reliability ε , desired average data rate \bar{R} , and spatial DoF m , where $m = \min\{M, N\}$. The embodiment of this relationship can be viewed as a performance bound of the spatiotemporal 2D channel coding to some extent.
- In the high SNR regime, this 2D channel coding rate can be simplified to a pretty concise format as

$$\frac{\bar{R}}{m} \leq \log_2(1 + \rho) - \sqrt{\frac{1}{mn}} \Phi^{-1}(\varepsilon), \quad (1)$$

where ρ represents the signal-to-noise ratio (SNR) and $\Phi^{-1}(\cdot)$ denotes the inverse of the Gaussian Q -function

$$\Phi(x) \triangleq \int_x^\infty \frac{1}{\sqrt{2\pi}} e^{-t^2/2} dt. \quad (2)$$

More interestingly, when the value of m is large enough, it turns out to be

$$n \approx \frac{m[\Phi^{-1}(\varepsilon)]^2}{[m\log_2(1+\rho) - \bar{R}]^2} \propto \frac{1}{m}, \quad (3)$$

which reveals an inversely proportional scaling law. That is, the latency in the time domain can be reduced by increasing the DoFs in the space domain, for the purpose of maintaining a certain level of performance target.

The remainder of this paper is organized as follows. The system model and relevant works are introduced in Section II. Section III presents a complete derivation of the expectation and variance for channel dispersion. The bounds on average maximal achievable rate are investigated in Section IV. Section V provides numerical results to reveal the potential relations of the most fundamental parameters involved in MIMO communications.

Notations: Boldface lower and upper case letters are used to denote vectors and matrices, respectively. The notation $(\cdot)^T$ and $(\cdot)^H$ denote the transpose and the conjugate transpose of a vector or matrix, respectively. We use \mathbf{I}_a to denote the identity matrix of size $a \times a$. The mean, variance, and probability of a random variable x are illustrated by the operators $\mathbb{E}\{x\}$, $\text{Var}\{x\}$, and $\mathbb{P}\{x\}$, respectively. The notation $\mathcal{CN}(0, \sigma^2)$ represents the complex Gaussian distribution with zero mean and variance σ^2 and $\mathcal{C}^{M \times N}$ denotes complex matrices with dimension $M \times N$. Moreover, we use $\text{tr}(\mathbf{A})$ and $\det(\mathbf{A})$ to denote the trace and determinant of matrix \mathbf{A} , respectively. The Frobenius norm of a matrix \mathbf{A} is denoted by $\|\mathbf{A}\|_F \triangleq \sqrt{\text{tr}(\mathbf{A}\mathbf{A}^H)}$. At last, for two functions $f(x)$ and $g(x)$, $f(x) = \mathcal{O}(g(x))$ means that $\limsup_{x \rightarrow \infty} |f(x)/g(x)| < \infty$.

II. SYSTEM MODEL

We consider an MIMO system with M transmit antennas and N receive antennas, operating over flat fading channels. Under the assumption that the synchronization is perfect and the channel is flat-fading quasi-static, the baseband equivalent discrete-time input-output relationship can be written as

$$\mathbf{Y} = \mathbf{H}\mathbf{X} + \mathbf{W}, \quad (4)$$

where $\mathbf{X} \in \mathcal{C}^{M \times n}$ is the signal transmitted over n time samples (channel uses), $\mathbf{Y} \in \mathcal{C}^{N \times n}$ is the corresponding received signal, and $\mathbf{H} \in \mathcal{C}^{N \times M}$ contains the complex fading coefficients, which are random but remain constant over the n time samples. It should be noted that this assumption for channel is usually reasonable for the case of uRLLC, due to the constrain of latency. When an *i.i.d.* Rayleigh fading channel is considered, each entry of \mathbf{H} is modelled as a Gaussian variable with zero mean and unit variance. $\mathbf{W} \in \mathcal{C}^{N \times n}$ denotes the additive noise at the receiver, which is independent of \mathbf{H} and also has *i.i.d.* $\mathcal{CN}(0, 1)$ entries.

According to [29], under the assumption of both isotropic codewords and perfect CSI at the receiver, the normal approximation to the maximal achievable rate is obtained as the solution of

$$\varepsilon = \mathbb{E} \left\{ \Phi \left[\frac{C(\mathbf{H}) - R^*(n, \varepsilon)}{\sqrt{V(\mathbf{H})/n}} \right] \right\}, \quad (5)$$

where n denotes the blocklength, ε represents the block error probability, and $\Phi^{-1}(\cdot)$ is the inverse of the Gaussian Q -function. $C(\mathbf{H})$ and $V(\mathbf{H})$ denote the Shannon capacity and channel dispersion conditioned on \mathbf{H} . When the transmitter has no CSI, it has been proved in [37] that the optimal power allocation should fulfill

$$\mathbf{X}\mathbf{X}^H = \frac{\rho}{M} \mathbf{I}_M. \quad (6)$$

In this case, the capacity and dispersion are further expressed as

$$C(\mathbf{H}) = \sum_{j=1}^m \log(1 + \rho\lambda_j/M) \quad (7)$$

and

$$V(\mathbf{H}) = m - \sum_{j=1}^m \frac{1}{(1 + \rho\lambda_j/M)^2}, \quad (8)$$

where λ_j denotes the j -th eigenvalue of $\mathbf{H}\mathbf{H}^H$ for $M \geq N$ and $\mathbf{H}^H\mathbf{H}$ for $M < N$.

III. STATISTICAL PROPERTIES OF CHANNEL DISPERSION

Since the channel matrix is random, its fading dynamics on the channel dispersion can be investigated by deriving its statistical properties. Specifically, its expectation, together with the capacity, can help us to analyze the average maximal achievable rate. As most of the practical systems work in the positive SNR regime, we consider in this paper only the case of $\rho > 0$.

A. Expectation

Taking expectation on (8), we obtain

$$\begin{aligned} \mathbb{E}\{V(\mathbf{H})\} &= \mathbb{E} \left\{ m - \sum_{j=1}^m \frac{1}{(1 + \rho\lambda_j/M)^2} \right\} \\ &= \mathbb{E} \left\{ m - \sum_{j=1}^m \frac{1}{1 + 2\rho\lambda_j/M + (\rho\lambda_j/M)^2} \right\} \\ &> \mathbb{E} \left\{ m - \sum_{j=1}^m \frac{1}{2\rho\lambda_j/M + (\rho\lambda_j/M)^2} \right\} \\ &= m - \mathbb{E} \left\{ \sum_{i=1}^m \frac{M^2/\rho^2}{\lambda_i(2M/\rho + \lambda_i)} \right\} \\ &= m - \frac{M}{2\rho} \mathbb{E} \left\{ \sum_{i=1}^m \frac{1}{\lambda_i} \right\} + \frac{M}{2\rho} \mathbb{E} \left\{ \sum_{i=1}^m \frac{1}{2M/\rho + \lambda_i} \right\}. \end{aligned} \quad (9)$$

According to [30, Eq. (41)], the first expectation on the right-hand-side (RHS) of (9) is obtained directly. That is,

i) $M > N$

$$\begin{aligned} \mathbb{E} \left\{ \sum_{i=1}^m \left(\frac{1}{\lambda_i} \right) \right\} &= \mathbb{E} \left\{ \text{tr}[(\mathbf{H}\mathbf{H}^H)^{-1}] \right\} \\ &= \frac{N}{M - N}, \end{aligned} \quad (10)$$

ii) $M < N$

$$\begin{aligned} \mathbb{E} \left\{ \sum_{i=1}^m \left(\frac{1}{\lambda_i} \right) \right\} &= \mathbb{E} \left\{ \text{tr} \left[(\mathbf{H}^H \mathbf{H})^{-1} \right] \right\} \\ &= \frac{M}{N - M}. \end{aligned} \quad (11)$$

The second expectation on the RHS of (9) can be derived by using the Stieltjes transform. The Stieltjes transform approach can solve most problems involved in random matrices, such as the distribution functions of the empirical eigenvalues of large random matrices [40], [41]. After some mathematical manipulations in Appendix A, we obtain its closed-form expression in (14) on the top of the next page.

From (10) and (11), we see that the sum of the reciprocals of eigenvalues is the power of the inverse of correlation matrix. However, it is somewhat striking that the expectation of this power does not exist when $M = N$ [39]. For this, we have to go back to the original expression of (9). Since $1 + \rho\lambda_j/M > 1$ for each eigenvalue, (9) can be derived by

$$\begin{aligned} \mathbb{E} \{V(\mathbf{H})\} &= \mathbb{E} \left\{ m - \sum_{j=1}^m \frac{1}{(1 + \rho\lambda_j/M)^2} \right\} \\ &> \mathbb{E} \left\{ m - \sum_{j=1}^m \frac{1}{1 + \rho\lambda_j/M} \right\} \\ &= m - \frac{M}{\rho} \mathbb{E} \left\{ \sum_{i=1}^m \frac{1}{M/\rho + \lambda_i} \right\}. \end{aligned} \quad (12)$$

By using the Stieljes transform and Marčenko-Pastur law, we obtain

$$\mathbb{E} \{V(\mathbf{H})\} = N + \frac{N}{2\rho} - \frac{N\sqrt{1+4\rho}}{2\rho}. \quad (13)$$

Fig. 1 gives comparison results of the channel dispersion for $N = M$. The analytical results are calculated according to (13). Most interestingly, although these expectations are derived for large numbers of antennas, they are also quite accurate for small-to-moderate antenna numbers in the high SNR regime. For notational simplicity, we therefore omit the limit operator in (14) on the top of next page.

Finally, by combining (10), (11), (13) and (14), we obtain the complete close-form expression for the expectation of channel dispersion. Most Interestingly, these expressions can be further simplified to some constant in some special cases. For example, in a massive MIMO system with $N = 1$, as M goes to infinity, we find

$$\lim_{M \rightarrow \infty} \mathbb{E} \left\{ \sum_{i=1}^m \frac{1}{2M/\rho + \lambda_i} \right\} = 0 \quad (15)$$

and

$$\lim_{M \rightarrow \infty} \frac{M}{2\rho} \mathbb{E} \left\{ \sum_{i=1}^m \left(\frac{1}{\lambda_i} \right) \right\} = \lim_{M \rightarrow \infty} \frac{M}{2\rho} \cdot \frac{1}{M-1} = \frac{1}{2\rho}. \quad (16)$$

In this case, the channel dispersion, for any positive SNR, can be approximated by

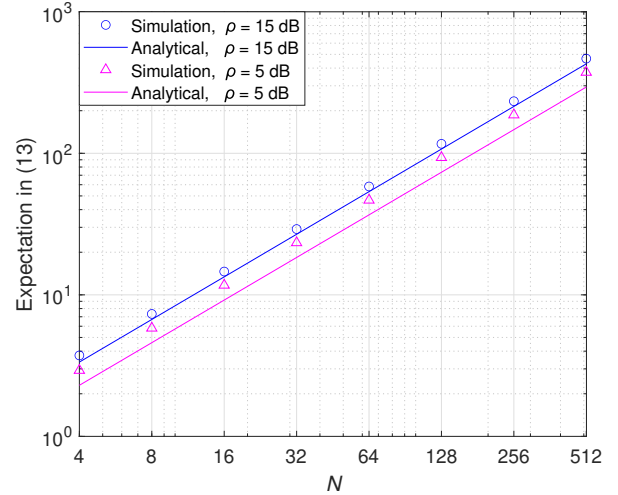


Fig. 1. Expectation comparison for $N = M$.

$$\lim_{M \rightarrow \infty} \mathbb{E} [V(\mathbf{H})] \approx 1 - \frac{1}{2\rho}. \quad (17)$$

B. Variance

The variance of channel dispersion is written by

$$\begin{aligned} \sigma_V^2 &= \mathbb{E} \left\{ (V(\mathbf{H}) - \mathbb{E}[V(\mathbf{H})])^2 \right\} \\ &= \mathbb{E} \left\{ \left(\sum_{j=1}^m \frac{1}{(1 + \rho\lambda_j/N_t)^2} \right)^2 \right\} \\ &\quad - \left[\mathbb{E} \left\{ \sum_{j=1}^m \frac{1}{(1 + \rho\lambda_j/N_t)^2} \right\} \right]^2. \end{aligned} \quad (18)$$

Since we already have the result of the second term of RHS in (18), the remaining task is to obtain the closed-form formula of the first term which has a denominator of order four. Unfortunately, it is difficult to calculate the high order moments of Wishart distributed matrices. Thus, we have to find some way to reduce the order and try to make use of the available results of their low order moments. Following this idea, the first term is bounded as follows

$$\mathbb{E} \left\{ \sum_{i=1}^m \frac{1}{2M/\rho + \lambda_i} \right\} = \begin{cases} \frac{N}{M} \left(\frac{\rho(NM - M^2)}{4N^2} - \frac{M}{2N} + \frac{\sqrt{(\rho M^2 - \rho MN + 2MN)^2 + 8\rho N^2 M^2}}{4N^2} \right) & N > M \\ \frac{\rho(NM - N^2)}{4M^2} - \frac{N}{2M} + \frac{\sqrt{(\rho N^2 - \rho MN + 2MN)^2 + 8\rho N^2 M^2}}{4M^2} & N < M \end{cases} \quad (14)$$

$$\begin{aligned} & \mathbb{E} \left\{ \left(\sum_{j=1}^m \frac{1}{(1 + \rho\lambda_j/M)^2} \right)^2 \right\} \\ &= \mathbb{E} \left\{ \left(\sum_{j=1}^m \frac{1}{1 + 2\rho\lambda_j/M + (\rho\lambda_j/M)^2} \right)^2 \right\} \\ &> \mathbb{E} \left\{ \left(\sum_{j=1}^m \frac{1}{2\rho\lambda_j/M + (\rho\lambda_j/M)^2} \right)^2 \right\} \\ &= \mathbb{E} \left\{ \left[\frac{M}{2\rho} \sum_{i=1}^m \left(\frac{1}{\lambda_i} - \frac{1}{2M/\rho + \lambda_i} \right) \right]^2 \right\} \\ &\triangleq G1 - 2 \cdot G2 + G3 + G4, \end{aligned} \quad (19)$$

where we define

$$G1 \triangleq \mathbb{E} \left\{ \left(\frac{M}{2\rho} \right)^2 \sum_{i=1}^m \left(\frac{1}{\lambda_i} \right)^2 \right\} \quad (20)$$

$$G2 \triangleq \mathbb{E} \left\{ \left(\frac{M}{2\rho} \right)^2 \sum_{i=1}^m \sum_{j=1}^m \frac{1}{\lambda_i (2M/\rho + \lambda_j)} \right\}, \quad (21)$$

$$G3 \triangleq \mathbb{E} \left\{ \left(\frac{M}{2\rho} \right)^2 \sum_{i=1, i \neq j}^m \frac{1}{\lambda_i \lambda_j} \right\}, \quad (22)$$

and

$$G4 \triangleq \mathbb{E} \left\{ \left(\frac{M}{2\rho} \right)^2 \sum_{i=1}^m \sum_{j=1}^m \frac{1}{(2M/\rho + \lambda_i)(2M/\rho + \lambda_j)} \right\}. \quad (23)$$

Now the original expression has been expanded to the sum of multiple parts which all have a lower order. Moreover, some of them already have closed-form results. Based on the properties of a Wishart Matrix introduced in [32, Lemma 2.10], for $M > N + 1$, we have

$$G1 = \left(\frac{M}{2\rho} \right)^2 \frac{MN}{(M - N)^3 - (M - N)}, \quad (24)$$

and

$$G3 = \left(\frac{M}{2\rho} \right)^2 \frac{N(N - 1)}{(M - N)(M - N + 1)}. \quad (25)$$

Unfortunately, it is difficult to derive the exact close-form expressions for G2 and G4 by using conventional integration approaches, since there is an additional term $2M/\rho$ appearing in the denominator. So, we resort to some approximations to

the original expression. Otherwise, even if it can be solved, it may comprise of some special functions which makes the expression less tractable. By taking an independence assumption between two elements of G2, we obtain its closed-form result, for $M > N + 1$, as

$$G2 = \zeta \left(\frac{M}{2\rho} \right)^2 \frac{N^2}{M - N} \left[\frac{N - M}{4\rho N} - \frac{1}{2} + \frac{\rho \sqrt{(M - N + 2N/\rho)^2 + 8N^2/\rho}}{4N} \right], \quad (26)$$

where $\zeta = 1/(\psi N)$ denotes the emendation parameter and ψ is a real number which varies with ρ .

Proof: See Appendix B.

Similar to the derivation of G2, we use the independence assumption and express G4, for the case of $M > N + 1$, as

$$G4 = \xi \left[\frac{M(N - M)}{8N} - \frac{M}{4\rho} + \frac{M \sqrt{(M - N + 2N/\rho)^2 + 8N^2/\rho}}{8N} \right]^2, \quad (27)$$

where ξ is also an emendation parameter varying with ρ .

When $N = M$, the expectation term in (15) can be rewritten as

$$\begin{aligned} & \mathbb{E} \left\{ \left(\sum_{j=1}^m \frac{1}{(1 + \rho\lambda_j/M)^2} \right)^2 \right\} \\ &< \mathbb{E} \left\{ \left(\sum_{j=1}^m \frac{1}{1 + \rho\lambda_j/M} \right)^2 \right\} \\ &= \left(\frac{M}{\rho} \right)^2 \mathbb{E} \left\{ \sum_{i=1}^m \sum_{j=1}^m \frac{1}{(M/\rho + \lambda_i)} \cdot \frac{1}{(M/\rho + \lambda_j)} \right\}. \end{aligned} \quad (28)$$

Expression in (28) has a form similar to G4, except for the scaling factor of two. By using the same mathematical tools and the independence assumption, we have

$$\mathbb{E} \left\{ \left(\sum_{j=1}^m \frac{1}{(1 + \rho\lambda_j/M)^2} \right)^2 \right\} < \frac{N^2 \xi}{4\rho^2} (\sqrt{1 + 4\rho} - 1)^2, \quad (29)$$

where ξ denotes the emendation parameter varying with ρ .

Fig. 2 shows simulation results of (28) for $N = M$. The analytical results are calculated according to (29). As we

know, the ordered eigenvalues in the random matrix are in fact correlated to each other, which introduces approximation errors. Fortunately, these approximation errors can be marginal by adjusting the emendation parameters, as shown in Fig 2.

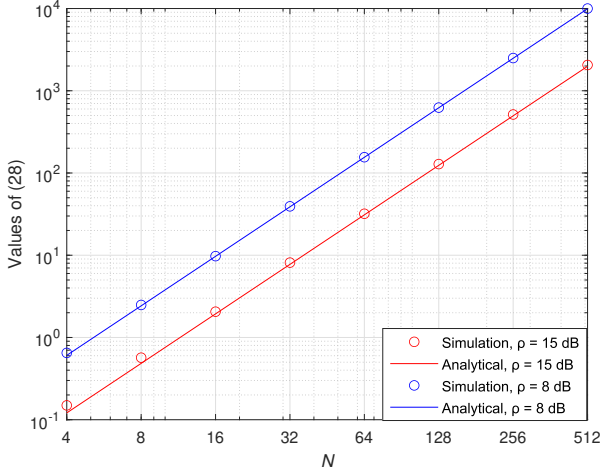


Fig. 2. Variance comparison for $N = M$.

IV. BOUNDS ON AVERAGE MAXIMAL ACHIEVABLE RATE

Since the variance of channel dispersion decreases largely as N goes to infinite, it can be treated as a deterministic number to some extent. In this case for small n , we have

$$\begin{aligned} \varepsilon &> \Phi \left[\mathbb{E} \left\{ \frac{C(\mathbf{H}) - R^*(n, \varepsilon)}{\sqrt{V(\mathbf{H})/n}} \right\} \right] \\ &= \Phi \left[\frac{\mathbb{E}\{C(\mathbf{H})\} - R^*(n, \varepsilon)}{\mathbb{E}\{\sqrt{V(\mathbf{H})/n}\}} \right]. \end{aligned} \quad (30)$$

As a result, the upper bound of the maximal average achievable rate can be written as

$$R^*(n, \varepsilon) < \bar{R} = \mathbb{E}[C(\mathbf{H})] - \sqrt{\frac{\mathbb{E}[V(\mathbf{H})]}{n}} \Phi^{-1}(\varepsilon), \quad (31)$$

where the expectation of channel dispersion can be found in (10), (11), (13), and (14). It should be noted that the big O term in (31) is neglected, since it has a relatively much smaller value, when compared with the capacity of massive MIMO systems.

Although these expressions are accurate, they seem to be so complicated that it is not convenient to use them in performance analysis. In fact, the results with concise expressions are more useful in studying the relationship between the blocklength and coding rate.

A. High SNR Regime

In the high per-antenna SNR regime, i.e., $\rho/M \gg 1$, the channel dispersion can be approximated as

$$\begin{aligned} \mathbb{E}\{V(\mathbf{H})\} &= m - \mathbb{E} \left\{ \sum_{j=1}^m \frac{1}{(1 + \rho \lambda_j/M)^2} \right\} \\ &\approx m - \frac{M^2}{\rho^2} \mathbb{E} \left\{ \sum_{j=1}^m \frac{1}{\lambda_j^2} \right\}. \end{aligned} \quad (32)$$

Based on the properties of Wishart matrix given in [32, Lemma 2.10], we obtain

$$\mathbb{E}[V(\mathbf{H})] \approx m - \frac{M^2}{\rho^2} \cdot \frac{NM}{(M-N)^3 - (M-N)}. \quad (33)$$

Interestingly, as the SNR per antenna goes to infinity, (33) is be further simplified approximately to

$$\mathbb{E}[V(\mathbf{H})] \approx m. \quad (34)$$

In some cases, if one of M and N is much larger than the other, (34) holds apparently for $\rho/M \gg 1$.

Proof: See Appendix C.

On the other hand, the capacity in the high SNR regime also has a simple approximated formula as [28]

$$\mathbb{E}[C(\mathbf{H})] \approx m \log(1 + \rho). \quad (35)$$

Consequently, a concise and analytically tractable expression for the average coding rate at a finite blocklength is achieved as

$$\bar{R} \approx m \log(1 + \rho) - \sqrt{\frac{m}{n}} \Phi^{-1}(\varepsilon). \quad (36)$$

B. Normalized Maximal Achievable Rate

As we know, after performing singular value decomposition (SVD) or eigenvalue decomposition, the MIMO channel can be transformed into multiple parallel orthogonal links. As a result, the average maximal achievable rate over all the links plays an important role in the performance analysis of massive MIMO systems at a finite blocklength. Following this idea, we divide (36) by m and obtain

$$\frac{\bar{R}}{m} \approx \log_2(1 + \rho) - \sqrt{\frac{1}{mn}} \Phi^{-1}(\varepsilon), \quad (37)$$

which can also be viewed as the rate bound of spatiotemporal 2D channel coding. Although the potential relations of the most fundamental parameters involved in MIMO communications has been revealed in many existing results, it is the first time to describe them in a concise and accurate closed-form expression. To gain a deep insight into the latency, we focus on n and m in the following analysis and let ρ and ε be any real positive numbers. Moreover, the channel matrix is assumed to be a square matrix with full rank, for the simplicity of analysis. In this case, from (37), we notice that the average data rate per Hz per antenna remains unchanged, when we fix the value of mn . This fact implies that n and m can be thought of being reciprocal to some extent and thus exchanging n by m is possible in theory. In

conventional MIMO systems, channel coding is conducted in the time domain on each link independently. So, if n decreases, the reliability can not be sustained any more, for a given coding rate. However, the observed reciprocal phenomenon suggests us that we can perform channel coding in the space domain along the links and exchange n by m to keep the total performance unchanged. Indeed, when the value of m is large enough, we obtain

$$n \approx \frac{m[\Phi^{-1}(\varepsilon)]^2}{[m\log_2(1+\rho) - \bar{R}]^2} \propto \frac{1}{m}, \quad (38)$$

which illustrates that latency is inversely proportional to the spatial DoF. This scaling law is just a basic principle behind the 2D channel coding presented in [10]. (38) also provides an upper bound for its maximal coding rate. More interestingly, it can be supposed that for an extreme case of $n = 1$, when m goes to infinity, the data rate per Hz per antenna, i.e. \bar{R}/m , approaches the Shannon capacity in AWGN channel.

V. NUMERICAL RESULTS AND ANALYSIS

Computer simulations were carried out in this section to verify the analytical results. We check the expectation of channel dispersion at first and then perform numerical results to study maximal achievable rate. Finally, the impact of imperfect CSI on the rate is investigated. In all the simulations, we set $c = N/M$.

A. Statistical Properties of Channel Dispersion

Fig. 3 gives numerical evaluation under different antenna configurations where the analytical results are calculated according to (10), (11), (13), and (14). It should be noted that in Fig. 3, although the analytical results coincide well with the simulation curves, there is still a visible small gap. The reason is that an ignorable term is omitted in the denominator of (9). Most strikingly, we find that (39) is accurate for all the dimensions of the matrix in the test. Figs. 4 and 5 give the simulation results to evaluate its accuracy. From both figures, the small gap diminishes by using (39).

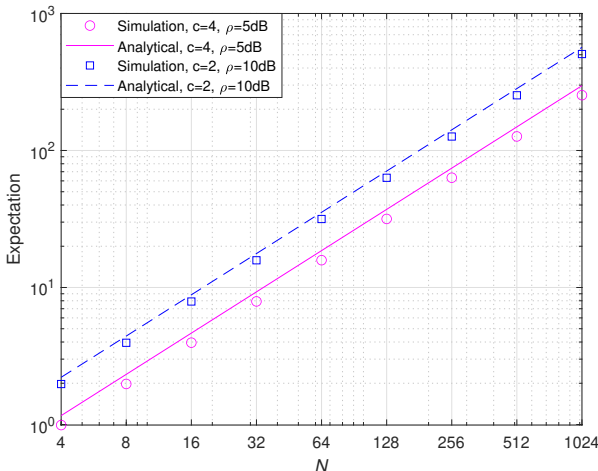


Fig. 3. Expectation of channel dispersion for $N > M$.

Then, we perform simulations to investigate the variance of channel dispersion. Fig. 6 illustrates the simulation results for different antenna configurations where the analytical results are calculated according to (24)-(27). The emendation parameters are set to $\psi = 57.5$ and $\xi = 0.5$ for $\rho = 5$ dB and $\psi = 370$ and $\xi = 0.6$ for $\rho = 7$ dB. As can be seen from Fig. 6 that the variance of channel dispersion is expected to be small, when compared with the expectation, which highlights the dominant role of expectation in the analysis of the system performance.

B. Normal Approximation

Fig. 7 shows the block error probability for the case of $\rho = 20$ dB and $c = 8$. For normalization, the maximal achievable rate is set to $6.5N$ bit/s/Hz, where N denotes the number of receive antennas. Simulation results are obtained by using (5), while the analytical results are calculated according to (30). As n grows to 50, the gap between simulation and analytical results becomes noticeable, even though the trends of these curves remain the same. This gap mainly comes from that channel capacity $C(\mathbf{H})$ which has a non-negligible variance. Fortunately, this offset can be fixed by subtracting a standard deviation of the channel capacity from (30). That is, the approximation for $n = 50$, can be rewritten by

$$\varepsilon \approx \Phi \left[\frac{\mathbb{E}\{C(\mathbf{H})\} - \sigma_C - R^*(n, \varepsilon)}{\mathbb{E}\{\sqrt{V(\mathbf{H})/n}\}} \right], \quad (40)$$

where σ_C denotes the standard deviation. According to [41], the channel capacity in our channel model obeys the Gaussian distribution with variance

$$\sigma_C^2 = -\log \left(1 - \frac{c \cdot \mu_F(z)^2}{[1 + c \cdot \mu_F(z)]^2} \right), \quad (41)$$

where

$$\mu_F(z) = \frac{1-c}{2cz} - \frac{1}{2c} - \frac{\sqrt{(1-c-z)^2 - 4cz}}{2cz} \quad (42)$$

and

$$z = -\frac{1}{\rho}. \quad (43)$$

As can be seen from Fig. 7, the analytical results match well with the numerical results especially in the regime of large N , when using (40) for $n = 50$.

C. Bounds on Average Maximal Achievable Rate

This subsection presents numerical results to depict the potential relationships among blocklength, error probability, coding rate, and spatial DoF, based on (31). Fig. 8 shows the average maximal achievable rate as a function of n and ε under $\rho = 15$ dB. Different values of m are set to generate multiple surfaces for comparison. From Fig. 8, we can see that as m increases, n becomes smaller for a given average rate and error probability, which verifies that the latency in the time domain can be compensated by the DoFs in the space domain.

$$\mathbb{E}\{V(\mathbf{H})\} = \begin{cases} M - \frac{M^2}{2\rho(N-M)} + \frac{M^2}{2\rho N} \left(\frac{\rho(NM-N^2)}{4M^2} - \frac{N}{2M} + \frac{\sqrt{(\rho N^2 - \rho MN + 2MN)^2 + 8\rho N^2 M^2}}{4M^2} \right) & N > M \\ N + \frac{N}{2\rho} - \frac{N\sqrt{1+4\rho}}{2\rho} & N = M \\ N - \frac{MN}{2\rho(M-N)} + \frac{N}{2\rho} \left(\frac{\rho(NM-M^2)}{4N^2} - \frac{M}{2N} + \frac{\sqrt{(\rho M^2 - \rho MN + 2MN)^2 + 8\rho N^2 M^2}}{4N^2} \right) & N < M \end{cases} \quad (39)$$

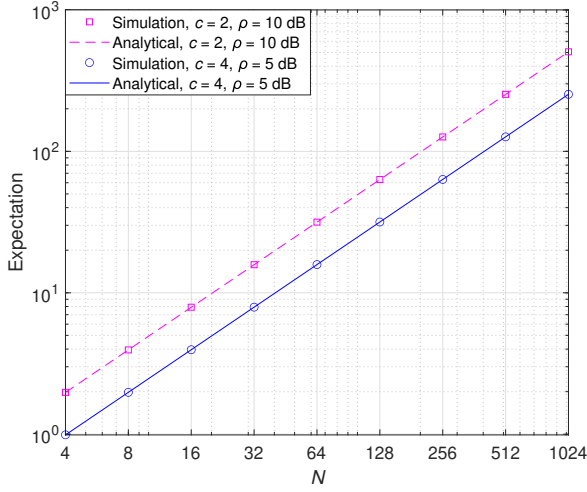
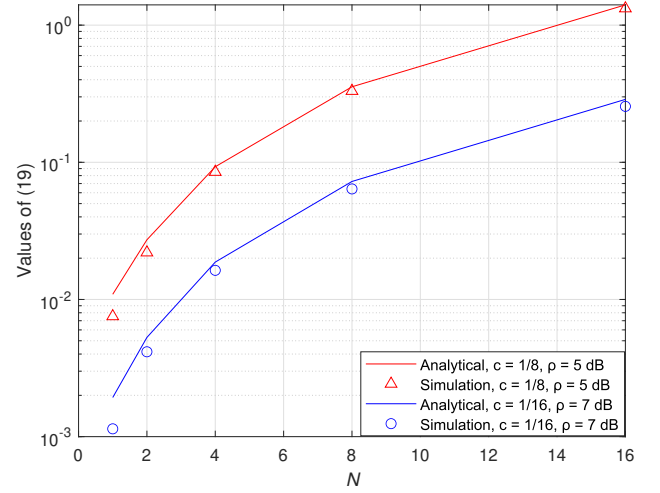
Fig. 4. Expectation of channel dispersion for $N > M$.

Fig. 6. Comparison of analytical and simulation results.

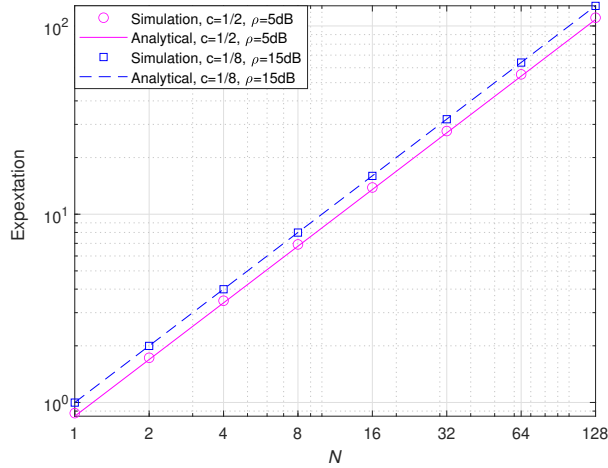
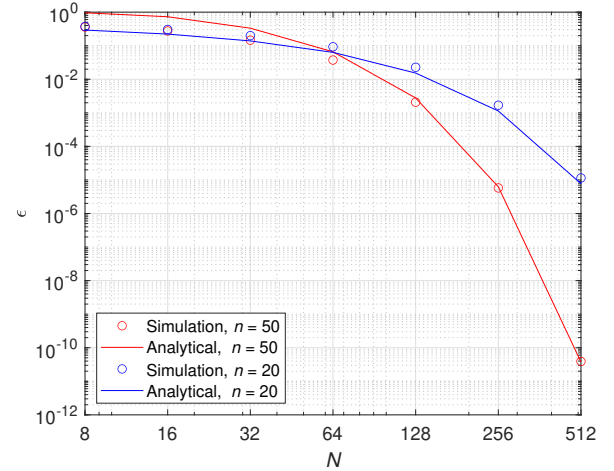
Fig. 5. Expectation of channel dispersion for $N < M$.

Fig. 7. Comparison of block error probability.

In Fig. 9, we fix the error probability at $\epsilon = 10^{-6}$ and vary n to compare their rates. In the tests, the SNR is set to $\rho = 15$ dB. From Fig. 9, all the curves approach the line of $\log_2(1 + \rho)$ as m increases and convergence speed accelerates as n grows. It is expected that when m goes to infinity, each link of the MIMO system can achieve the same Shannon capacity as that in an AWGN channel, for any positive blocklength.

In Fig. 10, the variance of \bar{R}/m is shown for $\epsilon = 10^{-6}$ and $n = 40$. From Fig. 10, we find that as the numbers of antennas at both transmitter and receiver increase, the variance of normalized average maximal achievable rate decreases quickly, analogous to the channel hardening phenomena in a massive

MIMO system. That is, as the DoF goes to infinite, the massive MIMO also reveals a feature of deterministic transmission, since the average maximal achievable coding rate per antenna is achieved at each transmission.

Moreover, we investigate the performance of error probability, as plotted in Fig. 11 with respect to m and n . With $\rho = 15$ dB and $\bar{R}/m = 4.95$. From Fig. 11, it suggests that we can either increase the blocklength or use more antennas at both transmitter and receiver to maintain a required reliability for a given rate and SNR.

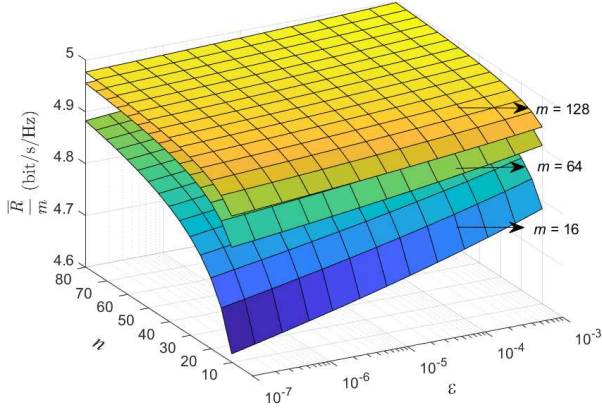
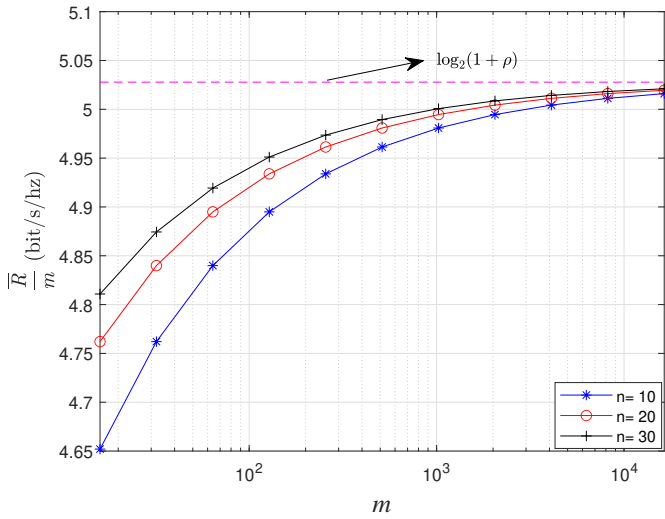


Fig. 8. Comparison of average rate for different DoFs.

Fig. 9. Comparison of average rate for different values of n .

D. Imperfect CSI

In practice, the CSI can be acquired by sending training symbols at transmitter. The training overhead is a function of the channel dynamics, because the faster the channel varies, the more training symbols are needed in order to estimate the channel accurately. According to [20] and [21], one way to determine the training overhead is to estimate the capacity penalty due to the lack of CSI. This makes it necessary to study the capacity in a noncoherent setting, where neither the transmitter nor the receiver are assumed to have the knowledge of CSI. The loss of capacity, when compared with the coherent setting, can be thought of as the minimum training overhead or cost of CSI at receiver. Interestingly, it has been reported in [22]–[24] that as SNR goes to infinity, the asymptotic ratio between the capacity and the logarithm of SNR approaches $1 - 1/T$, where T denotes the coherence time of the channel. It implies that the capacity penalty due to the lack of CSI at receiver diminishes when the channel coherence time is sufficiently large. In most practical systems, CSI is indispensable for coherent demodulation. When the mobility is relatively low, such as robots and autonomous vehicles in factory automation [43], there is usually enough time to send

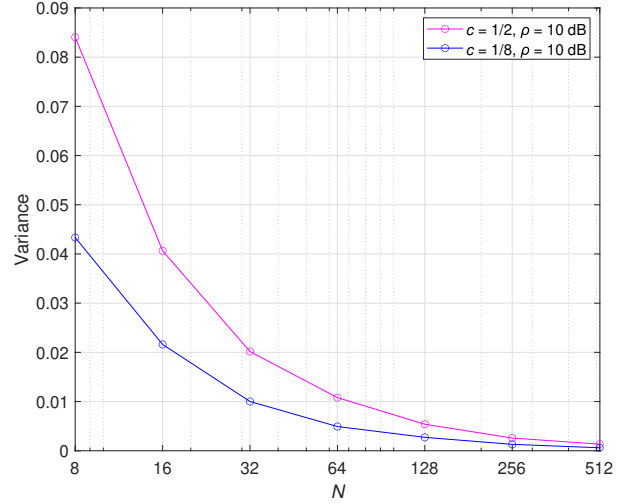
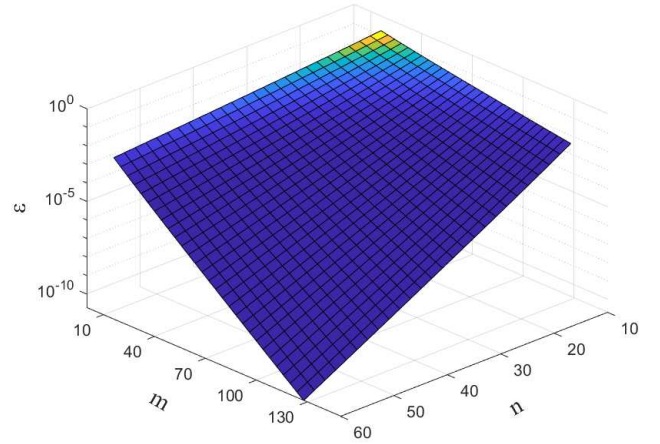
Fig. 10. Variance of average rate for different values of c .

Fig. 11. Comparison of blocklength for different DoFs.

pilots or training sequences. After the CSI is acquired, the following blocks within a period of coherence time can be used to carry data information. Even if the mobility is not low, some advanced channel estimation methods can still be used to predict the CSI, since the channel varies continuously in real environments [44].

When the situation of imperfect CSI is considered, the impact introduced by the channel estimate error is equivalently treated as an additional noise. In this case, its variance can be absorbed into the thermal noise, which reduces the SNR at the receiver, when compared with the perfect CSI scenario. Fig. 12 gives the simulation results of (31) with $\varepsilon = 10^{-5}$ and $n = 40$. From Fig. 12, as the variance of channel estimate error decreases, the loss in average maximal achievable rate becomes negligible. It should be noted that the overhead of training symbols is not considered directly in the derived expressions, because it mainly depends on the channel coherence time. If the coherence time is large enough, the rate penalty due to the transmission of known symbols at the receiver is expected to be ignorable [42].

In Fig. 13, the variance of the maximal achievable rate in

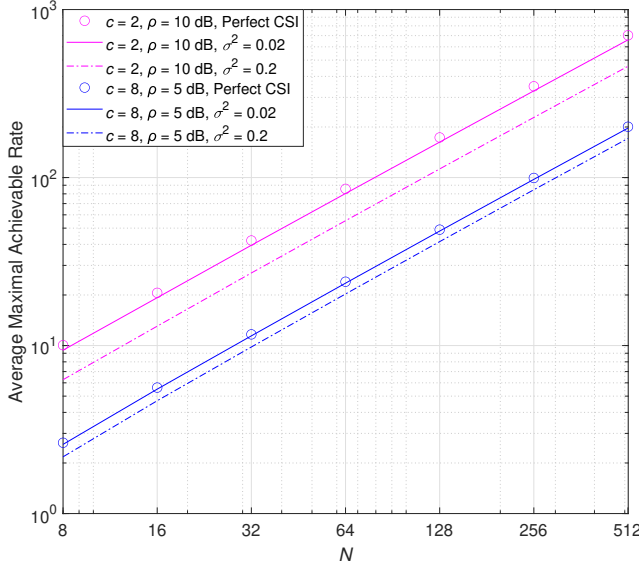


Fig. 12. Performance comparison with imperfect CSI.

(31) is tested by using the same parameters. Whether there is an channel estimation error or not, the variance of rate becomes smaller, as the number of antennas increases. In other words, the rate in each transmission approaches its expectation, just like the effect of channel hardening.

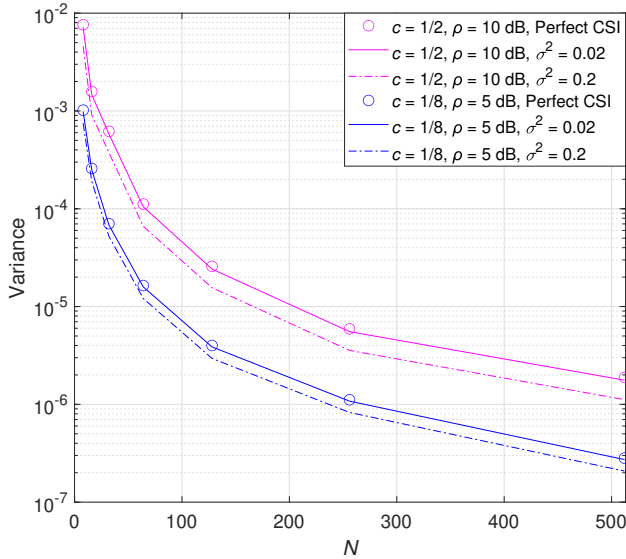


Fig. 13. Performance comparison with imperfect CSI.

VI. CONCLUSION

We have derived the closed-form expressions for channel dispersion in a massive MIMO scenario, which coincide well with the simulation results. Through using the obtain channel dispersions, the bound on maximal achievable rate at a finite blocklength can be expressed by a compact and precious formula in a normal approximation case which forms an unified framework to explore the relations among ϵ , n , R and

the number of spatial DoF. Based on the new framework, it is proved at the first time that, although most people think it is intuitively reasonable, coding along the space domain can also achieve the Shannon capacity, when the number of antennas goes to infinity. This gives rise a new methodology, named time space exchanging, to solve the contradictory problem between data rate and time latency.

APPENDIX

A. Proof of (14)

Let Λ be a diagonal matrix of eigenvalues of \mathbf{R} , where $\mathbf{R} = \mathbf{H}^H \mathbf{H}$ for the case of $N > M$. According to the definition of Stieltjes transform in [41], we have

$$\begin{aligned} \sum_{i=1}^m \frac{1}{2M/\rho + \lambda_i} &= \text{tr} \left[(\Lambda - z\mathbf{I}_m)^{-1} \right] \\ &= m \int \frac{1}{\lambda - z} dF^{\mathbf{R}}(\lambda), \end{aligned} \quad (44)$$

where $F^{\mathbf{R}}$ denotes the eigenvalue distribution function of \mathbf{R} and $z = -2M/\rho$. When m grows to infinity, it has been proved that $F^{\mathbf{R}}$ converges in distribution (often almost surely so) to some deterministic limit F , which can then be turned into approximative results for $F^{\mathbf{R}}$. Furthermore, by using Marčenko-Pastur law, the Stieltjes transform has a explicit expression as

$$\mu_F(z) = \frac{1-c}{2cz} - \frac{1}{2c} - \frac{\sqrt{(1-c-z)^2 - 4cz}}{2cz} \quad (45)$$

where $c = N/M$. Nevertheless, it should be noted that the entries of the matrices dealt with in this law have different variances with that of the elements in \mathbf{H} . So, the result of (45) should be scaled. Based on [32, Lemma 3.2], i.e.,

$$\mu_{a\mathbf{R}}(az) = \frac{1}{a} \mu_{\mathbf{R}}(z), \quad (46)$$

we obtain

$$\mu_F(z) = a \left(\frac{1-c}{2caz} - \frac{1}{2c} - \frac{\sqrt{(1-c-az)^2 - 4caz}}{2caz} \right), \quad (47)$$

where $a = c/M$. Since all the variables in this expression are deterministic, we say that the expectation approaches to

$$\begin{aligned} \lim_{M \rightarrow \infty} \mathbb{E} \left\{ \sum_{i=1}^m \frac{1}{2M/\rho + \lambda_i} \right\} &= \\ c \left(\frac{1-c}{2caz} - \frac{1}{2c} - \frac{\sqrt{(1-c-az)^2 - 4caz}}{2caz} \right). \end{aligned} \quad (48)$$

Finally, substituting $c = N/M$, $a = c/M$ and $z = -2M/\rho$ into (48) yields (14).

On the other hand, when $N \leq M$, (45) still holds. So, as long as we set $c' = 1/c$ and $a' = c'/M$ to scale the matrix, the expectation can then be obtained as

$$\lim_{M \rightarrow \infty} \mathbb{E} \left\{ \sum_{i=1}^m \frac{1}{2M/\rho + \lambda_i} \right\} = \left(\frac{1 - c'}{2c'a'z} - \frac{1}{2c'} - \frac{\sqrt{(1 - c' - a'z)^2 - 4c'a'z}}{2c'a'z} \right), \quad (49)$$

where $z = -2M/\rho$.

B. Proof of (26)

If all the eigenvalues are independent of each other, we can rewrite (21) as

$$\begin{aligned} \mathbb{E} \left\{ \left(\frac{M}{2\rho} \right)^2 \sum_{i=1}^m \sum_{j=1}^m \frac{1}{\lambda_i (2M/\rho + \lambda_j)} \right\} \\ = \left(\frac{M}{2\rho} \right)^2 \mathbb{E} \left\{ \sum_{i=1}^m \frac{1}{\lambda_i} \right\} \mathbb{E} \left\{ \sum_{j=1}^m \frac{1}{2M/\rho + \lambda_j} \right\}. \end{aligned} \quad (50)$$

Then, by using the results in (10) and (14), it is easy to obtain

$$\begin{aligned} \left(\frac{M}{2\rho} \right)^2 \mathbb{E} \left\{ \sum_{i=1}^m \frac{1}{\lambda_i} \right\} \mathbb{E} \left\{ \sum_{j=1}^m \frac{1}{2M/\rho + \lambda_j} \right\} \\ = \left(\frac{M}{2\rho} \right)^2 \frac{N^2}{M - N} \left[\frac{N - M}{4\rho N} - \frac{1}{2} \right. \\ \left. + \frac{\rho \sqrt{(M - N + 2N/\rho)^2 + 8N^2/\rho}}{4N} \right]. \end{aligned} \quad (51)$$

However, we all know that the eigenvalues are not independent in a matrix. They are actually correlated to each other. So, this expression is not accurate and needs to be emended. Fortunately, simulation results show that it has the same trend of variation as that of G2 and their difference can be corrected by a constant parameter. Thus, we finally obtain

$$\begin{aligned} \text{G2} = \zeta \left(\frac{M}{2\rho} \right)^2 \frac{N^2}{M - N} \left[\frac{N - M}{4\rho N} - \frac{1}{2} \right. \\ \left. + \frac{\rho \sqrt{(M - N + 2N/\rho)^2 + 8N^2/\rho}}{4N} \right], \end{aligned} \quad (52)$$

where $\zeta = 1/(\psi N)$ denotes the emendation parameter and ψ is a real number which has different values for different ρ .

C. Proof of (34)

At first, we consider $M > N$ and obtain

$$\begin{aligned} \mathbb{E}[V(\mathbf{H})] &\approx m - \frac{m}{\rho^2} \cdot \frac{M^3}{(M - m)^3 - (M - m)} \\ &= m \left(1 - \frac{1}{\rho^2} \cdot \frac{M^3}{(M - m)^3 - (M - m)} \right) \\ &= m \left(1 - \frac{1}{\rho^2} \cdot \text{G5} \right). \end{aligned} \quad (53)$$

In practical systems, the number of transmit antennas is usually set to be an integer multiple of the receive antennas, such as 5G downlink, to facilitate the use of multi-user MIMO or support coordinated multiple points (CoMP) transmissions. In this case, M is an even number and m ranges from 1 to $M/2$, i.e., $1 \leq m \leq M/2$. Substituting the extreme values into G5 and assuming $M > 2$, we obtain

$$\begin{aligned} \frac{M^3}{(M - m)^3 - (M - m)} &< \frac{M^3}{(M - \frac{M}{2})^3 - (M - 1)} \\ &= \frac{8M^2}{M^2 - 8 + \frac{8}{M}} < 13. \end{aligned} \quad (54)$$

In the high SNR regime, ρ is of course larger than $\sqrt{13}$. So,

$$\frac{1}{\rho^2} \cdot \text{G5} < 1 \quad (55)$$

holds obviously. When we further increase ρ to a very large number, the term in (53) diminishes completely and (34) is obtained then.

For the case of $M < N$, the bound of ρ to make G5 be smaller than one can be found by using the same way, but we would not repeat it here, due to the limited room.

REFERENCES

- [1] J. Sachs, G. Wikstrom, T. Dudda, *et al.*, "5G radio network design for ultra-reliable low-latency communication," *IEEE Network*, vol. 32, no. 2, pp. 24–31, 2018.
- [2] S. Liu, C. Zheng, Y. Huang, and T. Q. S. Quek, "Distributed reinforcement learning for privacy-preserving dynamic edge caching," *IEEE J. Sel. Areas Commun.*, vol. 40, no. 3, pp. 749–760, 2022.
- [3] 3rd Generation Partnership Project (3GPP), *Evolved Universal Terrestrial Radio Access (E-UTRA); Radio Resource Control (RRC); Protocol specification*, Technical Specification (TS) 36.331, 04 2017.
- [4] G. J. Sutton, J. Zeng, R. P. Liu, *et al.*, "Enabling technologies for ultra-reliable and low latency communications: From PHY and MAC layer perspectives," *IEEE Commun. Surv. Tutor.*, vol. 21, no. 3, pp. 2488–2524, 2019.
- [5] W. Xu, Y. Huang, W. Wang, F. Zhu, and X. Ji, "Toward ubiquitous and intelligent 6G networks: From architecture to technology," *Science China Information Sciences*, vol. 66, no. 3, pp. 5–6, Mar. 2023.
- [6] W. Saad, M. Bennis, and M. Chen, "A vision of 6G wireless systems: Applications, trends, technologies, and open research problems," *IEEE Network*, vol. 34, no. 3, pp. 134–142, 2019.
- [7] W. Xu, Z. Yang, D. W.-K. Ng, M. Levorato, Y. C. Eldar, and M. Debbah, "Edge learning for B5G networks with distributed signal processing: Semantic communication, edge computing, and wireless sensing," *IEEE J. Sel. Topics Signal Process.*, vol. 17, no. 1, pp. 9–39, Jan. 2023.
- [8] X. You, C. Wang, J. Huang, *et al.*, "Towards 6G wireless communication networks: Vision, enabling technologies, and new paradigm shifts," *Science China Information Sciences*, vol. 64, no. 1, pp. 1–74, 2021.
- [9] M. Giordani, M. Polese, M. Mezzavilla, S. Rangan, and M. Zorzi, "Toward 6G Networks: Use Cases and Technologies," *IEEE Commun. Mag.*, vol. 58, no. 3, pp. 55–61, Mar. 2020.
- [10] X. You, "6G extreme connectivity via exploring spatiotemporal exchangeability," *Science China Information Sciences*, vol. 66, no. 3, pp. 94–96, 2023.
- [11] Y. Liu, Y. Deng, M. Elkashlan, A. Nallanathan, and G. K. Karagiannis, "Analyzing grant-free access for URLLC service," *IEEE J. Sel. Areas Commun.*, vol. 39, no. 3, pp. 741–755, Mar. 2021.
- [12] C. She, Y. Duan, G. Zhao, T. Q. S. Quek, Y. Li and B. Vucetic, "Cross-layer design for mission-critical IoT in mobile edge computing systems," *IEEE Internet Things J.*, vol. 6, no. 6, pp. 9360–9374, Dec. 2019.
- [13] C. She, Z. Chen, C. Yang, T. Q. S. Quek, Y. Li and B. Vucetic, "Improving network availability of ultra-reliable and low-latency communications with multi-connectivity," *IEEE Trans. Commun.*, vol. 66, no. 11, pp. 5482–5496, Nov. 2018.

- [14] N. Bui, M. Cesana, S. A. Hosseini, Q. Liao, I. Malanchini and J. Widmer, "A survey of anticipatory mobile networking: Context-based classification, prediction methodologies, and optimization techniques," *IEEE Commun. Surv. Tutor.*, vol. 19, no. 3, pp. 1790–1821, Q3 2017.
- [15] C. E. Shannon, "A mathematical theory of communication," *Bell System Technical Journal*, vol. 27, pp. 379–423, 1948.
- [16] R. G. Gallager, *Information Theory and Reliable Communication*, New York, USA, Wiley, 1968.
- [17] X. You, "Shannon theory and future 6G's technique potentials," *Scientia Sinica Informationis*, vol. 50, no. 9, pp. 1377–1394, 2020.
- [18] Y. Polyanskiy, H. V. Poor, and S. Verdú, "Channel coding rate in the finite blocklength regime," *IEEE Trans. Inf. Theory*, vol. 56, no. 5, pp. 2307–2359, May 2010.
- [19] Y. Polyanskiy and S. Verdú, "Scalar coherent fading channel: Dispersion analysis," in *Proceedings of the IEEE International Symposium on Information Theory*, pp. 2959–2963, Aug. 2011.
- [20] W. Yang, G. Durisi, T. Koch, and Y. Polyanskiy, "Diversity versus channel knowledge at finite block-length," in *Proc. IEEE Information Theory Workshop*, pp. 572–576, Sept. 2012.
- [21] A. Lapidoth, "Diversity versus channel knowledge at finite block-length," *IEEE Trans. Inf. Theory*, vol. 51, no. 2, pp. 437–446, Feb. 2005.
- [22] B. M. Hochwald and T. L. Marzetta, "Unitary space-time modulation for multiple-antenna communications in Rayleigh flat fading," *IEEE Trans. Inf. Theory*, vol. 46, no. 2, pp. 543–564, Mar. 2000.
- [23] L. Zheng and D. Tse, "Communication on the Grassmann manifold: A geometric approach to the noncoherent multiple-antenna channel," *IEEE Trans. Inf. Theory*, vol. 48, no. 2, pp. 359–383, Feb. 2002.
- [24] G. Durisi and H. Bolcskei, "High-SNR capacity of wireless communication channels in the noncoherent setting: A primer," *Int. J. Electron. Commun. (AEU)*, vol. 65, no. 8, pp. 707–712, Aug. 2011.
- [25] A. Lancho, T. Koch, and G. Durisi, "On single-antenna Rayleigh block-fading channels at finite blocklength," *IEEE Trans. Inf. Theory*, vol. 66, no. 1, pp. 496–519, Jan. 2020.
- [26] B. Makki, T. Svensson, and M. Zorzi, "Finite block-length analysis of spectrum sharing networks using rate adaptation," *IEEE Trans. Commun.*, vol. 63, no. 8, pp. 2823–2835, Aug. 2015.
- [27] E. Telatar, "Capacity of multi-antenna Gaussian channels," *European Trans. Telecommun.*, vol. 10, no. 6, pp. 585–595, Dec. 1999.
- [28] L. Zheng and D. Tse, "Diversity and multiplexing: A fundamental tradeoff in multiple-antenna channels," *IEEE Trans. Inf. Theory*, vol. 49, no. 5, pp. 1073–1096, May 2003.
- [29] W. Yang, G. Durisi, T. Koch, and Y. Polyanskiy, "Quasi-static multiple-antenna fading channels at finite blocklength," *IEEE Trans. Inf. Theory*, vol. 60, no. 7, pp. 4232–4265, Jul. 2014.
- [30] B. Makki, T. Svensson, G. Caire, and M. Zorzi, "Fast HARQ over finite blocklength codes: A technique for low-latency reliable communication," *IEEE Trans. Wireless Commun.*, vol. 18, no. 1, pp. 194–209, Jan. 2019.
- [31] A. Collins and Y. Polyanskiy, "Dispersion of the coherent MIMO block-fading channel," in *Proc. IEEE International Symposium on Information Theory (ISIT)*, 2016, Barcelona, Spain, pp. 572–576.
- [32] J. Ostman, A. Lancho, G. Durisi, and L. Sanguinetti, "URLLC with massive MIMO: Analysis and design at finite blocklength," *IEEE Trans. Wireless Commun.*, vol. 20, no. 10, pp. 6387–6401, Oct. 2021.
- [33] A. Lancho, J. Ostman, G. Durisi, and L. Sanguinetti, "A finite-blocklength analysis for URLLC with massive MIMO," in *Proc. IEEE International Conference on Communications*, Montreal, QC, Canada, Jun. 2021.
- [34] A. Kislal, A. Lancho, G. Durisi, and E. Strom, "Efficient evaluation of the error probability for pilot-assisted URLLC with Massive MIMO," <https://arxiv.org/abs/2211.02385>.
- [35] C. Potter, K. Kosbar, and A. Panagos, "On achievable rates for MIMO systems with imperfect channel state information in the finite length regime," *IEEE Trans. Commun.*, vol. 61, no. 7, pp. 2772–2781, Jul. 2013.
- [36] T. L. Marzetta, "Noncooperative cellular wireless with unlimited numbers of base station antennas," *IEEE Trans. Wireless Commun.*, vol. 9, no. 11, pp. 3590–3600, Nov. 2010.
- [37] E. Abbe, S.-L. Huang, and I. E. Telatar, "Proof of the outage probability conjecture for MISO channels," *IEEE Trans. Inf. Theory*, vol. 59, no. 5, pp. 2596–2602, May 2013.
- [38] A. Lozano, A. M. Tulino, and S. Verdú, "Multiple-antenna capacity in the low-power regime," *IEEE Trans. Inf. Theory*, vol. 49, no. 10, pp. 2527–2544, Oct. 2003.
- [39] V. Jungnickel, T. Haustein, E. Jorswieck, and C. von Helmolt, "On linear pre-processing in multi-antenna systems," in *Proc. IEEE GLOBECOM*, Taiwan, China, pp. 1012–1016, Nov. 2002.
- [40] A. M. Tulino and S. verdú, *Random Matrix Theory and Wireless Communications*, Now Foundations and Trends, 2004.
- [41] R. Couillet and M. Debbah, *Random Matrix Methods for Wireless Communications*, Cambridge University Press, 2011.
- [42] D. Tse and P. Viswanath, *Fundamentals of Wireless Communication*, Cambridge University Press, 2005.
- [43] N. Jayaweera, D. Marasinghe, N. Rajatheva, and M. Latva-aho, "Factory automation: resource allocation of an elevated LiDAR system with URLLC requirements," in *Proc. 2nd 6G Wireless Summit (6G SUMMIT)*, Levi, Finland, Mar. 2020.
- [44] B. Yang, K. Letaief, R. Cheng, and Z. Cao, "Channel estimation for OFDM transmission in multipath fading channels based on parametric channel modeling," *IEEE Trans. Commun.*, vol. 49, no. 3, pp. 467–479, Mar. 2001.